Rapporto Tecnico INSEAN / Technical Report / 2006-085

Description of the INSEAN E779A Propeller Experimental Dataset

Francesco Salvatore, Francisco Pereira, Mario Felli,
Danilo Calcagni, Fabio Di Felice

INSEAN - Italian Ship Model Basin
Via di Vallerano, 139 - 00128 Rome (Italy)

ISBN: 978-88-7617-051-5 (e-book - pdf)

Publisher: Institute of Marine Engineering CNR-INM, National Research Council of Italy
(formerly INSEAN *Istituto Nazionale per Studi ed Esperienze di Architettura Navale*)

www.inm.cnr.it

DOI: 10.5281/zenodo.6077997

Report classification sheet

Title: **Authors:** **Department:**	Description of the INSEAN E779A Propeller Experimental Dataset F. Salvatore, F. Pereira, M. Felli, D. Calcagni, F. Di Felice Propulsion and Cavitation
Report number: **Version:** **Date:** **Number of pages:** **Key-words:**	2006-085 1 June 2006 35 + 6 Marine Propulsion, Propeller hydrodynamics, Propeller hydroacoustics, Cavitation, Experimental Techniques, LDV velocimetry, PIV velocimetry, Dataset for validation of CFD codes
Reference Contracts: **Confidentiality**	EU-FP6 Research Project VIRTUE; Project TIP5-CT-2005-516201 Distribution restricted to members of the VIRTUE Project Consortium
Abstract:	This report describes the INSEAN E779A Propeller dataset, a collection of experimental data on propeller hydrodynamics and hydroacoustics. The dataset includes a thorough description of propeller performance and of propeller-induced flowfield and pressure field over a variety of flow conditions realized during open water as well as cavitation tunnel tests. Propeller slipstream flow is characterized by means of advanced LDV and PIV techniques, whereas cavitation patterns are described via an innovative digital technique. In view of its completeness, the INSEAN E779A Propeller dataset represents a unique source of data for the validation of CFD codes. In this report, experimental data are presented and described. Presentation is oriented to direct use for numerical codes validation excercises. With minor modifications, this report is also available as "VIRTUE" Project Deliverable D4.1.3.

Contents

Report classification sheet **i**

List of Figures **iii**

List of Tables **iv**

1 Introduction **1**

2 Content of the INSEAN E779A Dataset **1**

3 Propeller in uniform inflow **2**

3.1 Open water characteristics 3

3.2 Velocity distribution in the propeller wake 5

3.2.1 Propeller wake flow measurements using LDV 5

3.2.2 Propeller wake flow measurements using PIV 8

3.3 Cavity pattern 12

4 Propeller in artificially generated wake **17**

References **23**

A The INSEAN E779A model propeller **25**

B Description of experimental facilities **30**

B.1 The towing tank 30

B.2 The cavitation tunnel 30

B.2.1 Description of wake generator for transient cavitation studies 31

C The INSEAN E779A Dataset CD-ROM **34**

List of Figures

1 The INSEAN E779A propeller: bronze model and mathematical description (IGES). . 2
2 Open water characteristics of the*INSEAN E779A* propeller. 4
3 LDV measurements: distribution of u_{RMS} on transversal planes at varying axial distance from the propeller plane (plane axial location increases from left to right, top to bottom). 7
4 PIV measurements: distribution of u_{RMS} on longitudinal plane $\theta = 0°$ at different advance coefficients: from top to bottom $J = 0.748, 0.88, 1.012$. 11
5 Map of cavitation types on the*INSEAN E779A* propeller. 13
6 Measured extension of sheet cavity on the*INSEAN E779A* propeller: cavity area A_C is presented as a fraction of a blade surface reference area, $A_0 = 0.460R_P^2$. 16
7 Sketch of the set-up with wake generator, propeller and pressure sensors: pressure transducers (P1, ..P4) and hydrophones (H1, ..H4). 18
8 Axial velocity distribution by LDV in the wake generated the plate array. Nominal wake (left) and total wake (right). 18
9 Attached cavity extension (mean value and fluctuations) referred to blade angular position θ: low tunnel pressure conditions (left) and high tunnel pressure conditions (right). Cavity area A_C is presented as a fraction of a blade surface reference area, $A_0 = 0.460R_P^2$. 20
10 Pressure transducers P1, P2, P3, P4: amplitudes A_k from Eq. 6 for the first four PBF harmonics and $2.5 < \sigma_0 < 7.5$. 22
11 *INSEAN E779A* model propeller drawings. Left: expanded outline; right: developed sectional profiles at correct pitch and rake. Dimensions in millimeters. 26
12 Tunnel set-up with propeller and wake generator. 32
13 Sketch of wake generator: details of plate rack (top) and set-up with propeller (bottom). The lower drawing is qualitative and horizontal and vertical dimensions are not correctly scaled; only indicated measures are correct. 33

List of Tables

1 Testing conditions for open water propeller measurements in the INSEAN towing tank. 3
2 INSEAN E779A open water chracteristics: measured loads (top) and coefficients of polynomial fit $f(x) = a_0 + a_1 J + a_2 J^2 + ...a_5 J^5$ (bottom). 3
3 Comparison of propeller loads at different Reynolds number in the range $J = 0.873 \pm 0.002$. (Different values of kinematic viscosity are used: $\nu = 1.1099 \times 10^{-6}$ [m^2/s] for towing tank data and $\nu = 1.01 \times 10^{-6}$ [m^2/s] for cavitation tunnel data.) 4
4 LDV measurements of propeller wake (non-cavitating, uniform flow) 6

5 PIV measurements of propeller wake (non-cavitating, uniform flow) 9

6 Cavitation on propeller in uniform flow: flow conditions and measured data. From top to bottom: $J = 0.71, 0.77, 0.83$. 15

7 Basic geometrical data of the*INSEAN E779A* model propeller. 25

8 Blade characteristics of the*INSEAN E779A* model propeller. 26

9 Blade sectional offsets of the*INSEAN E779A* model propeller: Non-dimensional chordwise abscissa ξ, back side offset y_B and face side offset y_F, in millimeters. Chordwise abscissae from $\xi = 0$ to $\xi = 0.2$. 27

10 Blade sectional offsets of the*INSEAN E779A* model propeller: Non-dimensional chordwise abscissa ξ, back side offset y_B and face side offset y_F, in millimeters. Chordwise abscissae from $\xi = 0.25$ to $\xi = 0.7$. 28

11 Blade sectional offsets of the*INSEAN E779A* model propeller: Non-dimensional chordwise abscissa ξ, back side offset y_B and face side offset y_F, in millimeters. Chordwise abscissae from $\xi = 0.75$ to $\xi = 1.0$. 29

12 Main characteristics of INSEAN Towing Tank No. 2. 30

13 Main characteristics of the Italian Navy cavitation tunnel (CEIMM). 31

1 Introduction

This report describes an experimental dataset on marine propeller hydrodynamics that is under development by INSEAN, the Italian Ship Model Basin, in the framework of various research programs. Related research was started in 1997 and is continuously carried on by INSEAN researchers.

The dataset described here is named *INSEAN E779A* after the reference code used to identify the propeller model utilized for all the experimental activity.

The dataset includes a thorough description of propeller performance and of propeller-induced flowfield and pressure field over a variety of flow conditions realized during open water as well as cavitation tunnel tests. Propeller slipstream flow is characterized by means of advanced LDV and PIV techniques, whereas cavitation patterns are described via an innovative digital technique. Operating conditions include propeller in uniform flow and propeller in non-uniform inflow generated by a suitable wake generator device.

In view of its completeness, the INSEAN E779A Propeller dataset represents a unique source of data for the validation of CFD codes. This report is intended to provide adequate description of the dataset in order to evaluate the selection of the dataset as a major test case for the validation of propeller cavitation codes that are under development in the framework of the research project *'VIRTUE'*.

In the present report, the dataset content is described and partially presented through pictures and tables where measured physical quantities and testing flow conditions are specified. In addition, measurement techniques and testing facilities are described, and a complete description of the propeller model geometry is given.

In order to facilitate the utilization of the dataset content for both validation and benchmarking activities within the VIRTUE project, experimental data are made available to partners via a CD-ROM, whose structure is illustrated in Appendix C.

2 Content of the INSEAN E779A Dataset

The *INSEAN E779A* dataset represents an extensive documentation of experimental activity aiming to determine propeller performance and to characterize the flowfield around the propeller under different conditions.

Three different operating conditions are considered:

- single propeller in uniform flow;
- single propeller in artificially generated wake;

The model propeller used during all the experimental activity is depicted in Fig. 1. It is a four-bladed, fixed-pitch, right-handed propeller characterized by a nominally constant pitch distribution

and very low skew. Propeller drawings and a complete definition of the propeller geometry is given in Appendix A.

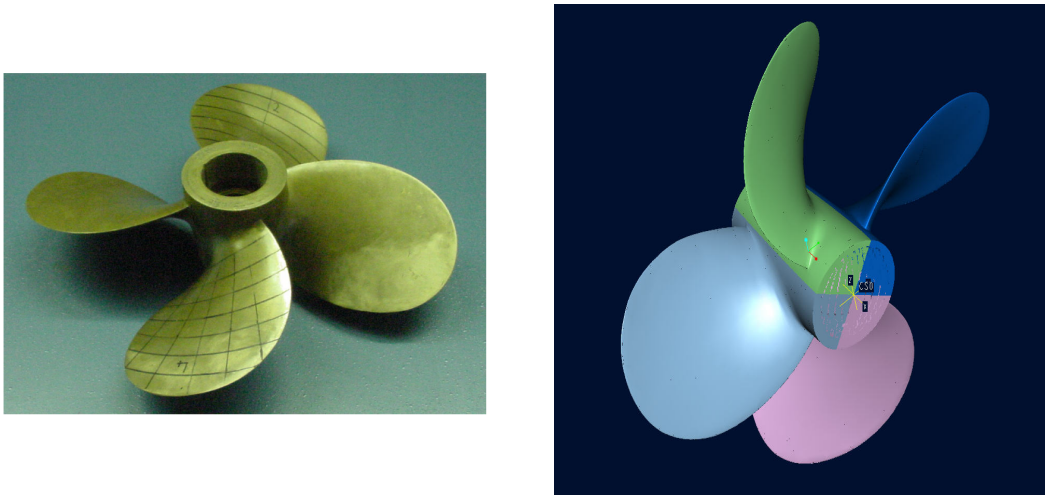

Figure 1: The INSEAN E779A propeller: bronze model and mathematical description (IGES).

An accurate description of the model geometry has been obtained through a three-dimensional mapping using a digital topometry technique developed by GOM m.b.H. (Germany). This technique allows to determine the shape of an arbitrary three-dimensional object with a very high precision. For the present case, a model propeller with diameter $D_P = 227.27mm$, the model surface is determined with a tolerance of $\pm 0.01mm$. Such tolerance allows to describe important shape details as the blade leading edge, trailing edge and tip with a sufficient precision. As a result of the digital mapping, a mathematical description of the 3D surface of the propeller in IGES format has been obtained. The propeller geometry descriptions in Appendix A have been determined by a post-processing of the 3D description in the IGES format. The IGES file of the propeller geometry is included in the *INSEAN E779A* CD-ROM, see Appendix C.

The experimental activity originating the *INSEAN E779A* dataset is being performed by INSEAN researchers in two facilities:

- *INSEAN medium-size towing tank*: open water curves;
- *Italian Navy cavitation tunnel (CEIMM)*: all other quantities.

For completeness, a description of these two facilities is given in Appendix B.

3 Propeller in uniform inflow

Experimental data on the INSEAN E779A model propeller in uniform flow conditions include:

- open water characteristics
- velocity distribution in the propeller wake
- pressure fluctuations
- cavitation inception, extent and character

3.1 Open water characteristics

Single propeller open water curves are obtained by tests performed at the INSEAN medium-size towing tank (see Appendix B for details). Testing conditions are given in Table 1.

Propeller revolution rate	11.7881 [rps]
water temperature	16.0 $^{\circ}C$
water density	102.6 [Kg s^2/m^4]
water viscosity	1.1099$\times 10^{-6}$ [m^2/s]

Table 1: Testing conditions for open water propeller measurements in the INSEAN towing tank.

Measured propeller thrust and torque coefficients

$$K_T = \frac{T}{\rho n^2 D_P^4}; \qquad K_Q = \frac{Q}{\rho n^2 D_P^5} \tag{1}$$

are given in Table 2 and plotted in Fig. 2 (both raw data and sixth-order polynomial fits are presented).

J	0.000	0.099	0.149	0.199	0.249	0.298	0.348	0.397	0.447
K_T	0.533	0.508	0.491	0.472	0.452	0.430	0.408	0.387	0.363
K_Q	0.0871	0.0829	0.0800	0.0771	0.0739	0.0707	0.0674	0.0641	0.0608
J	0.498	0.546	0.596	0.646	0.695	0.747	0.795	0.845	0.895
K_T	0.340	0.317	0.292	0.269	0.245	0.222	0.198	0.174	0.150
K_Q	0.0574	0.0541	0.0506	0.0472	0.0438	0.0405	0.0368	0.0332	0.0294
J	0.945	0.946	0.970	0.995	1.020	1.045	1.094	1.145	1.194
K_T	0.124	0.125	0.111	0.098	0.084	0.072	0.046	0.017	-.012
K_Q	0.0254	0.0255	0.0234	0.0215	0.0194	0.0176	0.0135	0.0088	0.0040

	a_0	a_1	a_2	a_3	a_4	a_5
K_T	0.53304	-0.19001	-0.76203	1.00701	-0.63301	0.14061
K_Q	0.087171	-0.036009	-0.101168	0.156295	-0.113664	0.028527

Table 2: INSEAN E779A open water chracteristics: measured loads (top) and coefficients of polynomial fit $f(x) = a_0 + a_1 J + a_2 J^2 + ...a_5 J^5$ (bottom).

Propeller thrust and torque are determined after zero balance values are obtained subtracting thrust and torque measured on a bladeless hub running at identical rotational speed.

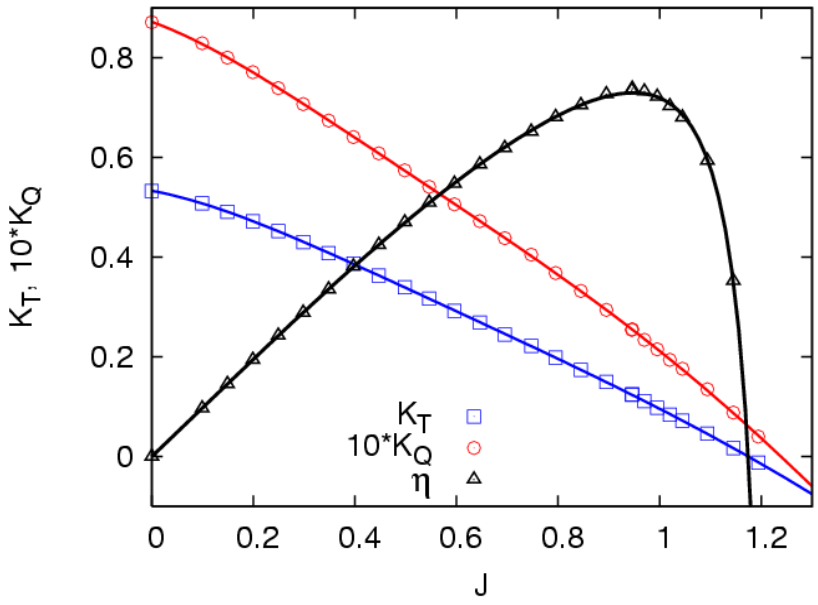

Figure 2: Open water characteristics of the *INSEAN E779A* propeller.

Different values of the advance coefficient have been obtained varying the towing velocity and keeping the propeller rotational speed constant, $n = 11.79$ rps. These testing conditions correspond to a constant Reynolds number, $Re_n = 5.49 \times 10^5$, where $Re_n = nD_P^2/\nu$ denotes the Reynolds number based on propeller rotational speed and diameter.

Additional tests were performed in order to quantify the effect of the Reynolds number on measured loads. In particular, for a fixed value of the advance coefficient, $J = 0.873 \pm 0.002$, measurements were repeated for different values of propeller rotational speed, and compared with measurements at higher rps performed in the cavitation tunnel (see Section 3.3, below). Measured thrust coefficients are compared in Table 3, where also the Reynolds number based on total inflow velocity at 70% blade radius is considered: $Re_{0.7R} = C_{0.7R}/\nu\sqrt{(2\pi n 0.7R_P)^2 + U_\infty^2}$, where $C_{0.7R}$ is the lenght of blade chord at 70% radius ($C_{0.7R} = 0.086$ m for the INSEAN E779A model propeller).

facility	n [rps]	J	$Re_n \times 10^{-6}$	$Re_{0.7R} \times 10^{-6}$	K_T	K_Q
towing tank	5.94	0.873	0.276	0.247	0.154	0.0300
towing tank	11.79	0.874	0.549	0.491	0.159	0.0310
towing tank	17.73	0.875	0.825	0.739	0.159	0.0311
cav. tunnel	36.00	0.871	1.841	1.647	0.165	0.0329

Table 3: Comparison of propeller loads at different Reynolds number in the range $J = 0.873 \pm 0.002$. (Different values of kinematic viscosity are used: $\nu = 1.1099 \times 10^{-6}$ [m^2/s] for towing tank data and $\nu = 1.01 \times 10^{-6}$ [m^2/s] for cavitation tunnel data.)

This analysis shows that Reynolds number effects are not negligible in the range of propeller rotational

speed used during open water tests. This is due to the laminar portion of the boundary layer at the blade leading edge. Its extension depends on the local Reynolds number and in particular is reduced as Re_n tends to increase. A typical means to limit this effect consists in using turbulence stimulators at the blade leading edge to force transition of laminar into turbulent flow. Such technique is not used in the experimental activity here described.

The variability of propeller thrust and torque with respect to Reynolds number is typically encountered during open water tests in towing tanks on medium size propeller models. Some comments on this subject may be found, *i.e.*, in the Report of the Propulsion Committee of the 23^{rd} ITTC [12].

3.2 Velocity distribution in the propeller wake

The *INSEAN E779A* dataset includes an extensive documentation of the propeller wakefield using advanced velocimetry techniques. Both Laser-Doppler Velocimetry (LDV) and Particle-Image Velocimetry (PIV) have been used. Details on the application of LDV techniques to propeller flow measurements at INSEAN are given *e.g.*, in references [2] and [3], whereas PIV techniques are described *e.g.*, in [4] and [8]. In addition, references [9] and [10] present a comparison between LDV and PIV methodologies.

The aim of these types of measurements is to provide a thorough investigation of the flow in the slipstream of a propeller. In particular, the dynamics of the vorticity generated on propeller blades and responsible for thrust generation can be described with high accuracy.

Velocimetry techniques like LDV and PIV allow to describe the propeller tip vortex flow, the slipstream contraction downstream the propeller, and the interaction among trailing vortices shed by different blades. The effect of viscosity-induced diffusion of trailing vorticity can also be accurately described.

Propeller flow measurements using LDV and PIV are described in the following two subsections. For convenience, both a cylindrical coordinate system (x, r, θ) and a Cartesian coordinate system (x, y, z) are introduced.

In particular, x is the longitudinal coordinate, aligned with the propeller axis and pointing downstream. The propeller disc plane is located at $x = 0$. The coordinate z is vertical and pointing from bottom to top, and y is defined in order to let (x, y, z) be a right-handed orthogonal coordinate system. Radial and tangential coordinates r, θ are defined on planes that are normal to the propeller axis (transversal planes). The radial coordinate r is pointing from propeller hub to tip, whereas the tangential coordinate θ is clockwise oriented as seen from downstream and is $\theta = 0$ in the twelwe o'clock position.

3.2.1 Propeller wake flow measurements using LDV

Laser-Doppler velocimetry has been largely used to characterize the the propeller wake flow through measurements at the CEIMM cavitation tunnel.

Available data for non-cavitating propeller in uniform inflow are summarized in Table 4.

Velocity is measured on five transversal planes downstream the propeller. On each transversal plane, measurement points are distributed on a polar grid.

flow conditions	$U_\infty = 5$ m/s, $n = 25$ rps ($J = 0.88$) (U_∞ measured by pitot-probe upstream the test section)
Measured region	5 transversal planes: $x/R_P = 0.20, 0.65, 1.15, 1.65, 2.15$ spanned area: $0.25R_P < r < 1.05R_P$ (approximately)
Measured quantitities	axial, radial, tangential velocity components
Derived quantitities	root mean square (RMS) of axial, radial, tangential velocity components

Table 4: LDV measurements of propeller wake (non-cavitating, uniform flow)

On the three planes closer to the propeller disk, $x/R = 0.20, 0.65, 1.15$, a total of 2160 points are distributed along 12 circumferences at radial positions between $r = 0.25R_P$ and $r = 1.05R_P$ ($R_P = D_P/2 = 113.635$ mm).

On the other two planes, $x/R = 1.65, 2.15$, 1980 points are distributed along 11 circumferences at radial positions between $r = 0.25R_P$ and $r = 1.0R_P$.

In all five planes, 180 points are distributed on each circunference with constant angular distance of $\Delta\theta = 2$ degrees.

The LDV technique used allows to measure three components of the flow velocity:

U_x [m/s]: total velocity in axial direction, positive if pointing downstream;

U_r [m/s]: total velocity along radial direction, positive in direction of increasing r;

U_θ [m/s]: total velocity in tangential direction, positive in counterclockwise direction as seen from downstream.

Velocity values are obtained by averaging over a very large number of data samples. Specifically, up to 10^3 pointwise raw data per propeller revolution are obtained, and acquisition is repeated for several propeller revolutions. Sampled data are tagged with blade angular position and allocated into angular slots of width $\Delta\theta_{slot} = 2^\circ$. Then, velocity values at a measured point identified by cylindrical coordinates (x_P, r_P, θ_P), are obtained by averaging all data samples tagged into the angular slot centered at θ_P and delimited by $\theta_P - \theta_{slot}/2 \leq \theta \leq \theta_P + \theta_{slot}/2$.

Statistical analysis on measured raw data allows to determine mean values as well as root mean square (RMS) values of the three velocity components. Mean value $\bar{U}_x$ and RMS $\hat{U}_x$ of the velocity component U_x are evaluated using the following definitions:

$$\bar{U}_x = \frac{1}{N_s}\sum_{n=1}^{N_s} U_{x_n}; \qquad \hat{U}_x = \frac{1}{N_s}\sum_{n=1}^{N_s}\sqrt{\left(U_{x_n} - \bar{U}_x\right)^2}, \tag{2}$$

where N_s is the number of data samples tagged with each slot. Similar definitions apply for mean values and RMS of velocity components U_y and U_z.

The RMS of velocity components have an important physical meaning in that they represent velocity fluctuations and can be related to the turbulent nature of the flowfield.

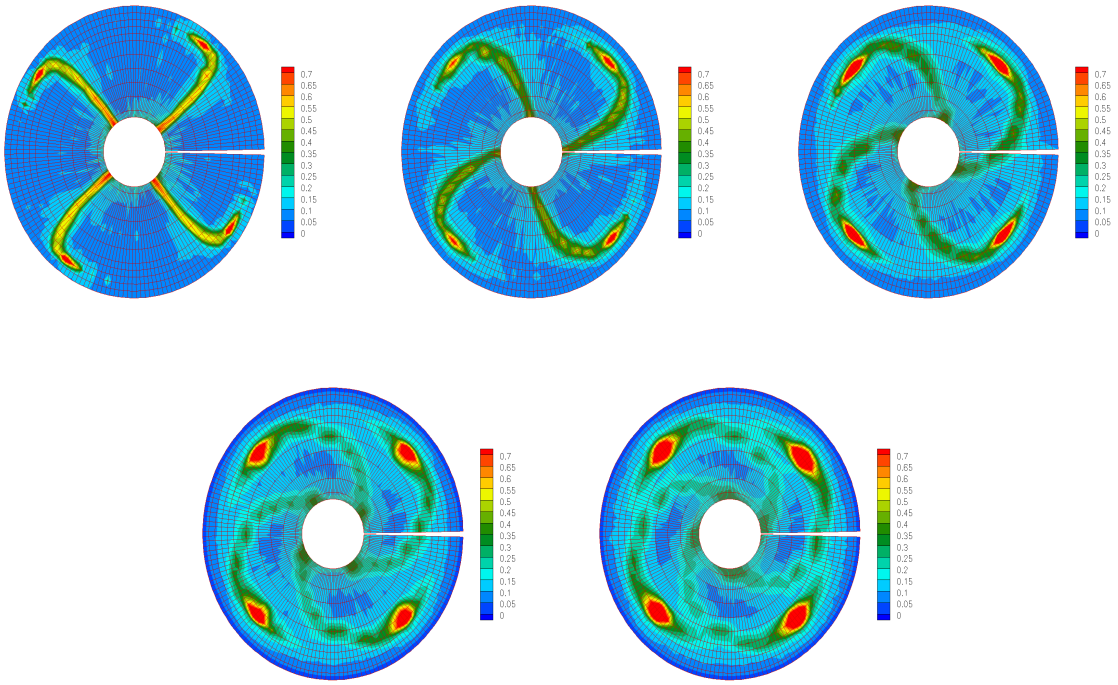

Figure 3: LDV measurements: distribution of u_{RMS} on transversal planes at varying axial distance from the propeller plane (plane axial location increases from left to right, top to bottom).

After processing of raw data, all the three velocity components are made non-dimensional with respect to the nominal inflow speed, U_∞. Measured velocity field is then presented as non-dimensional perturbation velocity components,

axial velocity: $u_x = (U_x - U_\infty)/U_\infty$

radial velocity: $u_r = U_r/U_\infty$

tangential velocity: $u_\theta = U_\theta/U_\infty$

As an example, the distribution of u_{RMS} at all the five planes is presented here through contour plots, see Fig. 3. The measurement grid is also shown in the Figures above.

Description of LDV data in the CD-ROM

In view of the large amount of data corresponding to LDV measurements of the propeller wake flow, these data are collected into the *INSEAN E779A* dataset CD-ROM (see Appendix C) and are not repeated in the present report.

Three different types of LDV data files are presented in the *INSEAN E779A* dataset CD-ROM. Raw data are given in text files and layouts ready for contour plots using TECPLOT©10 are also given:

- files with extension ".dat"
  formatted text files where raw data of measured quantities are stored. A TECPLOT©10 header is included. Each ".dat" files provides the following quantities:
  - 'teta', angular position θ, clockwise oriented as seen from downstream and zero in the twelve o'clock position;
  - 'r/R', adimensional radial position r/R_p, pointing from propeller hub to tip;
  - 'U', non-dimensional total velocity in axial direction U_x, and positive if pointing downstream;
  - 'V', non-dimensional perturbation velocity in radial direction u_r, (see above definition) and positive if pointing from propeller hub to tip;
  - 'W', non-dimensional perturbation velocity in tangential direction u_θ, (see above definition) and positive in counterclockwise direction as seen from downstream.
  - 'RMS(U)', that represents the root mean square of axial velocity component, non-dimensional;
  - 'RMS(V)', that represents the root mean square of radial velocity component, non-dimensional;
  - 'RMS(W)', that represents the root mean square of tangential velocity component, non-dimensional;
- files with extension ".lay"
  , TECPLOT©10 files created to present data in graphical format; these files read ".plt" files in input;
- files with extension ".plt"
  , TECPLOT© 10 unformatted, binary files; these files contain in a different format the information contained in ".dat" files.

Using TECPLOT©10 layouts, the user should take care of adjusting contour levels when changing the plotted quantity.

3.2.2 Propeller wake flow measurements using PIV

Particle-Image Velocimetry measurements of the propeller wake flow documented in the *INSEAN E779A* dataset are summarized in Table 5.

Measurement planes (x, r, θ_n) are equally spaced in circumferential direction between $\theta_0 = 0°$ and $\theta_{18} = 85°$, with angular step $\Delta\theta = 5°$.

On each plane, measurement points are uniformly distributed on rectangular areas corresponding to the *interrogation windows* that are processed in one step by the PIV set-up cameras (see details in [4]). Throughout these windows, measurement points are equally spaced with $\Delta x = \Delta r = .007189 R_P$, corresponding to pixel size.

Flow conditions	three values: $J = 0.748, 0.88, 1.012$
Measured region	18 longitudinal planes (x, r, θ_n) at different θ_n locations (all J values) (spanned area: *see details below*)
Measured quantitities	axial, radial velocity components
Derived quantitities	root mean square (RMS) of axial, radial velocity components vorticity component in the (x, r, θ_n) plane

Table 5: PIV measurements of propeller wake (non-cavitating, uniform flow)

A total of 45764 pixels distributed on three interrogation windows have been considered to study the two cases $J = 0.748$ and $J = 1.012$, whereas 76276 pixels distributed on five interrogation windows have been considered at $J = 0.88$. This corresponds to the following extension of the measured regions on each plane:

- $J = 0.748$ and $J = 1.012$:
  $0.1225R_P < x < 2.8022R_P$; $0.16R_P < r < 1.05R_P$ (approximately);
- $J = 0.88$:
  $0.1225R_P < x < 4.5824R_P$; $0.16R_P < r < 1.05R_P$ (approximately).

A small blank area is present between two successive interrogation windows. In addition, windows are not exactly aligned, and a small shift in radial direction is present. Length of both axial and radial shifts are of the same order of magnitude as the pixel size.

Pointwise velocity values are obtained as an average of the flow velocity within control areas whose area equals the pixel size and are associated to measurement points that are defined as the centroids of the control areas.

Acquisitions for each interrogation window are repeated to perform statistical analysis on data. Mean values and root mean square (RMS) values of the following in-plane velocity components are then provided (see description of LDV data elaboration):

- u_x: non-dim. perturbation velocity along axial direction, positive if pointing downstream;
- u_r: non-dim. perturbation velocity along radial direction, positive in direction of increasing r.

As a post-processing, also the in-plane vorticity component ω_θ is determined by taking finite differences of measured velocity components u_x and u_r. Although vorticity ω_θ is not a direct output of measurements, it still represent a highly reliable information in that velocity data are provided on a fine grid and hence numerical errors related to finite differencing of data from direct measurements introduce a small error.

As an example, the distribution of u_{RMS} at a representative plane ($\theta = 0$) is presented here through contour plots, see Fig. 4.

Description of PIV data in the CD-ROM

In view of the large amount of data corresponding to PIV measurements of the propeller wake flow, these data are collected into the *INSEAN E779A* dataset CD-ROM (see Appendix C) and are not repeated in the present report.

Similarly to LDV data, three different types of PIV data files are presented in the *INSEAN E779A* dataset CD-ROM:

- files with extension ".dat"
  formatted text files where raw data of measured quantities are stored. A TECPLOT©10 header is included. Each ".dat" files provides the following quantities:
  - 'x/R', non-dimensional axial position x/R_p, positive in downstream direction;
  - 'y/R', non-dimensional radial position r/R_p, pointing from inner to outer radii;
  - 'U/Uinf', non-dimensional total velocity in axial direction U_x/U_∞ and positive if pointing downstream;
  - 'V/Vinf', non-dimensional perturbation velocity in radial direction U_r/U_∞ and positive if pointing from propeller hub to tip;
  - 'RMS(U)/Uinf', root mean square of axial velocity component, non-dimensional with respect to U_∞;
  - 'RMS(V)/Uinf', root mean square of radial velocity component, non-dimensional with respect to U_∞;
  - 'vorticity', in-plane vorticity component ω_θ (this quantity is set equal to zero).
- files with extension ".lay"
  , TECPLOT©10 files created to present data in graphical format; these files read ".plt" files in input;
- files with extension ".plt"
  , TECPLOT©10 unformatted, binary files; these files contain in a different format the information contained in ".dat" files.

Using TECPLOT©10 layouts, the user should take care of adjusting contour levels when changing the plotted quantity.

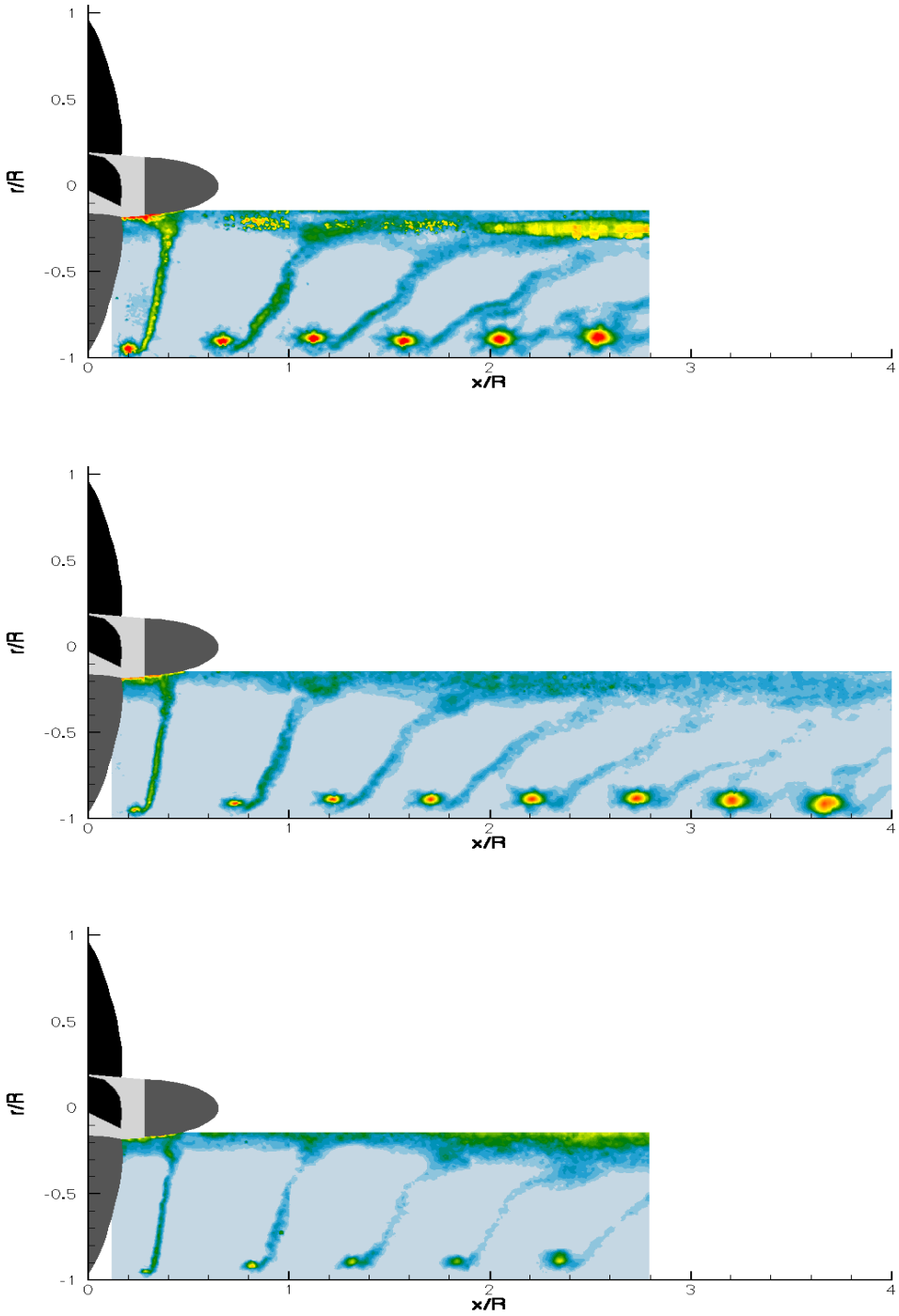

Figure 4: PIV measurements: distribution of u_{RMS} on longitudinal plane $\theta = 0°$ at different advance coefficients: from top to bottom $J = 0.748, 0.88, 1.012$.

3.3 Cavity pattern

The experimental investigation of cavitation on the *INSEAN E779A* model propeller represents a major contribution of the present dataset. Experimental data include both uniform flow conditions (discussed here below) as well as propeller in artificially-generated wake, as described in Section 4. The experimental analysis of propeller cavitation has been performed at the Italian Navy cavitation tunnel (CEIMM, see Appendix B).

A complete characterization of cavitation phenomena over a wide range of propeller operating conditions is achieved using high-speed camera visualizations combined with propeller loads measurements and (only for unsteady flow analysis) propeller-induced noise measurements.

An advanced digital image processing technique is then used to provide quantitative information on blade cavity location and extension. Details on the digital image technique are given in [14] and [15].

Considering a propeller in uniform inflow, different operating conditions are obtained varying both the advance coefficient J and tunnel pressure. Two adimensional parameters are used here to define pressure conditions: cavitation number σ_n based on propeller rotational speed, and cavitation number σ_0 based on freestream axial velocity,

$$\sigma_n = \frac{p_\infty - p_V}{\frac{1}{2}\rho(nD)^2}; \qquad \sigma_0 = \frac{p_\infty - p_V}{\frac{1}{2}\rho U_\infty^2}. \tag{3}$$

In Eq. (3), p_∞ and p_V denote, respectively, free-stream pressure (measured upstream the tunnel test section) and vapour pressure (referred to tunnel operating conditions). Recalling $J = U_\infty/nD$, yields $\sigma_0 = \sigma_n/J^2$.

Testing at different J and σ_n allows to investigate the effect of blade loading and field pressure on cavitation, and a variety of two phase flow appearances are observed. This is reflected in Fig. 5, where different types of cavitation observed are associated with corresponding flow conditions in terms of J and σ_n.

Typical cavitation trends of old-design propellers having low skew and loaded blade tip are recovered. It can be noted that both bubble cavitation, attached sheet cavitation (partial cavitation) and supercavitation is present. Vaporization occurs only on the blade suction side: no face cavitation is documented. In most cases, the sheet cavity attached to the blade surface merges at the blade tip with a vaporized region which developes into a cavitating tip-vortex. At relatively high pressure and light loading conditions, leading edge cavitation is observed. Some streak cavitation occurrences at very low pressure are observed at mid span. These features are likely related to local shape defects at the blade leading edge of the aged model propeller used.

Among all the flow conditions observed, a representative number of cases have been selected and described in detail in the present report. The following quantities are given:

- propeller rotational speed n [RPS], freestream velocity U_∞ [m/s], advance coefficient J;
- cavitation number σ_n, Reynolds number $Re_{0.7R} = C_{0.7R}V_{0.7R}/\nu$;

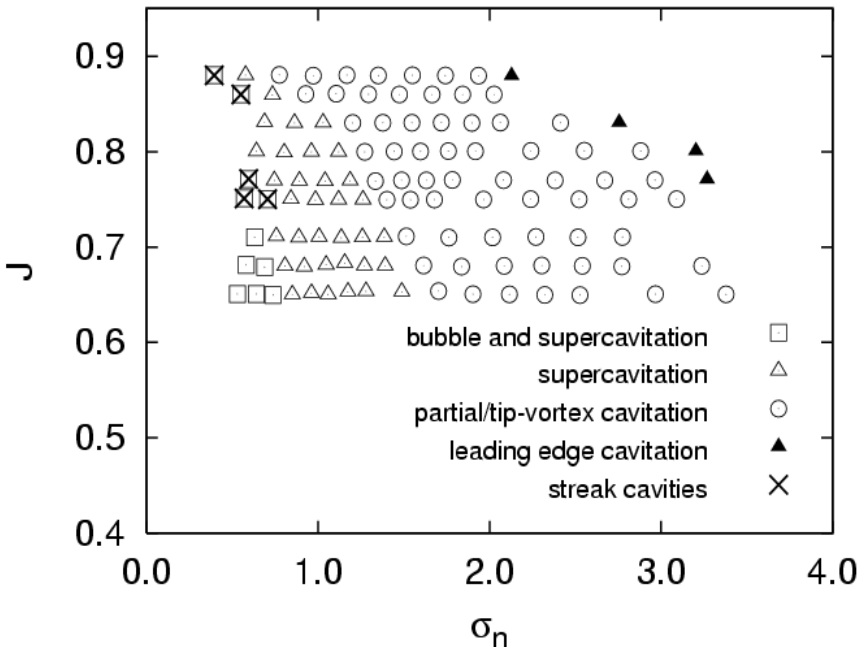

Figure 5: Map of cavitation types on the *INSEAN E779A* propeller.

- propeller thrust T, torque Q and corresponding coefficients K_T, K_Q;
- cavity area A_C (mean value and standard deviation, see Eq. (4));
- high-resolution pictures of blade cavitation.

Experimental results are given in the *INSEAN E779A* dataset CD-ROM (see Appendix C). Here, some representative data are summarized in Table 6, and in Fig. 6.

Three values of advance coefficient, $J = 0.83,\ 0.77,\ 0.71$ are obtained by varying the inflow speed whereas the propeller rotational speed is kept almost constant at 36 rps; the corresponding Reynolds number $Re_{0.7R}$ is slightly varied between 1.60 and 1.62 millions (kinematic viscosity of water $\nu = 1.01 \times 10^{-6}$ m^2/s).

For each value of J, pressure is varied from non-cavitating conditions (highest σ_n value) to strong cavitation (lowest σ_n recorded values). Lower pressure conditions than those indicated in Table 6 have not been studied because of difficulty to achieve stable and repeatable conditions in the tunnel.

Cavity area is determined using the digital image processing technique described by Pereira et al. in [14]. For each flow condition, a preliminary observation of cavity patterns on the four blades is made and the blade presenting the most repeatable behaviour is chosen as the reference blade. This allows to avoid measurement uncertainty related to differences among propeller blades.

Once the reference blade is tagged, about 150 digital images are taken and processed to perform a statistical analysis on measured data. Cavity area mean value $\bar{A}_C$ and standard deviation $\hat{A}_C$ are

defined as (N_s denoting the number of data samples):

$$\bar{A}_C = \frac{1}{N_s}\sum_{n=1}^{N_s} A_{C_n}; \qquad \hat{A}_C = \frac{1}{N_s}\sum_{n=1}^{N_s}\sqrt{\left(A_{C_n} - \bar{A}_C\right)^2} \tag{4}$$

Both mean values and standard deviation are then adimensionalized with respect to a reference area, A_0, defined as the area of the propeller blade back side between radial section at $r/R_P = 0.36$ and blade tip ($A_0 = 0.460R_P^2$.), see Fig. 6.

n [rps]	35.99	35.99	36.00	36.01	36.01	36.01	36.02	36.01	36.02	36.02	36.02	36.02	36.02
U_∞ [m/s]	5.808	5.814	5.807	5.813	5.805	5.810	5.812	5.818	5.809	5.812	5.815	5.811	5.814
σ_n	0.630	0.757	0.888	1.007	1.136	1.259	1.386	1.515	1.764	2.018	2.270	2.516	2.775
$\bar{A}_C/A_0$	0.387	0.348	0.303	0.268	0.233	0.205	0.174	0.149	0.120	0.093	0.074	0.060	0.049
$\hat{A}_C/A_0$	1.308	1.563	0.714	0.791	0.699	0.558	0.365	0.360	0.254	0.253	0.301	0.405	0.345
K_T	0.216	0.229	0.241	0.249	0.254	0.254	0.255	0.255	0.255	0.256	0.255	0.255	0.256
10 K_Q	0.405	0.426	0.445	0.456	0.463	0.463	0.462	0.460	0.460	0.461	0.461	0.462	0.464

n [rps]	36.03	35.61	35.61	35.61	35.61	35.62	35.62	35.62	35.61	35.61	35.61	35.61	35.61	36.02
U_∞ [m/s]	6.312	6.227	6.223	6.224	6.225	6.223	6.230	6.230	6.232	6.231	6.230	6.230	6.231	6.309
σ_n	0.596	0.745	0.891	1.042	1.188	1.335	1.487	1.632	1.783	2.082	2.382	2.672	2.964	3.268
$\bar{A}_C/A_0$	0.410	0.275	0.225	0.188	0.155	0.128	0.109	0.088	0.077	0.054	0.041	0.032	0.029	0.027
$\hat{A}_C/A_0$	6.998	2.340	0.988	0.956	1.109	0.441	0.593	0.463	0.404	0.339	0.406	0.145	0.189	0.167
K_T	0.199	0.212	0.221	0.223	0.224	0.224	0.224	0.224	0.224	0.224	0.224	0.225	0.224	0.224
10 K_Q	0.379	0.401	0.415	0.418	0.417	0.417	0.416	0.417	0.417	0.417	0.418	0.420	0.419	0.417

n [rps]	36.02	35.61	35.61	35.61	35.61	35.60	35.60	35.61	35.61	35.61	35.61
U_∞ [m/s]	6.800	6.715	6.716	6.716	6.717	6.717	6.719	6.716	6.718	6.719	6.719
σ_n	0.688	0.864	1.029	1.202	1.378	1.547	1.719	1.897	2.063	2.413	2.756
$\bar{A}_C/A_0$	0.181	0.131	0.099	0.078	0.064	0.051	0.042	0.036	0.030	0.023	0.019
$\hat{A}_C/A_0$	0.470	0.638	0.402	0.391	0.334	0.252	0.168	0.221	0.289	0.234	0.149
K_T	0.189	0.192	0.192	0.192	0.192	0.192	0.192	0.192	0.192	0.192	0.192
10 K_Q	0.363	0.368	0.368	0.367	0.368	0.368	0.369	0.370	0.370	0.370	0.370

Table 6: Cavitation on propeller in uniform flow: flow conditions and measured data. From top to bottom: $J = 0.71, 0.77, 0.83$.

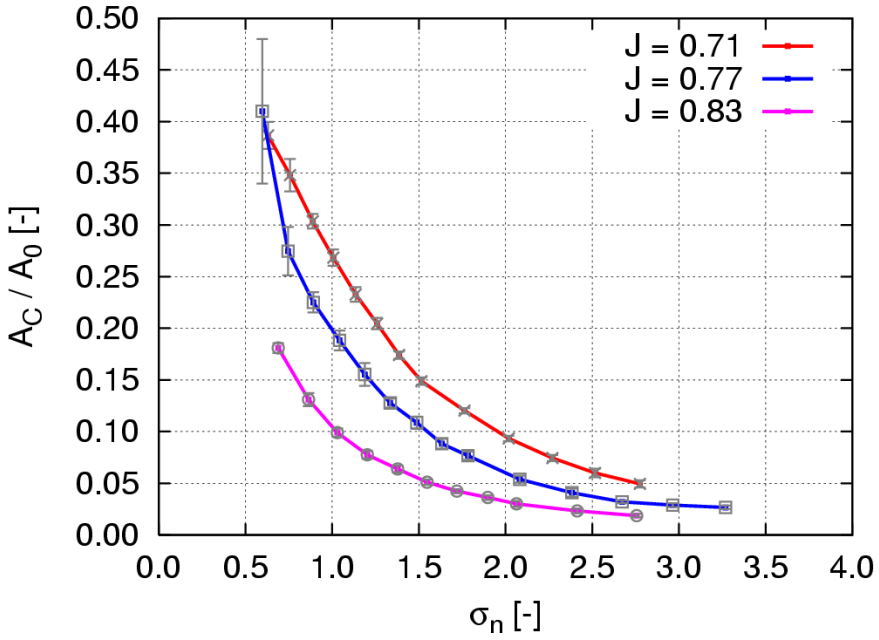

Figure 6: Measured extension of sheet cavity on the *INSEAN E779A* propeller: cavity area A_C is presented as a fraction of a blade surface reference area, $A_0 = 0.460 R_P^2$.

Propeller thrust and torque measurements performed at varying cavitation number allow to describe cavitation-induced loads breakdown under very low pressure conditions.

Measured K_T and K_Q are corrected in order to take into account flow confinement effects in the cavitation tunnel. Recalling the *INSEAN E779A* propeller model has $R_P = 0.11364$ m, a blocking factor $b = \pi R_P^2 / A_{tunnel} = 0.11$ is obtained. Under these testing conditions, a correction of measured propeller loads to eliminate flow confinement effects is applied in the range of 2-3%, or $(K_T)_{O.W.} = 0.97 \div 0.98 (K_T)_{tunnel}$. It is worth to stress that all the experimental data from tunnel tests documented in the present report include such a confinement effect correction based on approximated theoretical assumptions, see *e.g.*, [11].

In view of the correction applied, K_T and K_Q values at highest σ_n presented in Table 6 (corresponding to cavitation-free conditions) are comparable to open water measurements at the same advance coefficient presented in Section 3.1. Discrepancies between these two sets of data are motivated by the fact that measurements have been obtained running the propeller model at different Reynolds numbers. In particular, open water curves in Section 3.1 correspond to $Re_n = 5.49 \times 10^5$, whereas K_T and K_Q values at highest σ_n from Table 6 correspond to $Re_n = 16.75 \times 10^5$. In such a range of variation of the Reynolds number, viscosity effects on measured propeller loads are not negligible, as illustrated in Table 3 (see, *e.g.* [12]).

4 Propeller in artificially generated wake

Recent experimental activity on the INSEAN E779A model propeller has been primarily devoted to complete the characterization of the propeller flow considering non-uniform flow conditions.

Measurements include:

- inflow to propeller
- propeller loads
- cavitation patterns
- pressure fluctuations

A major feature is that quantitative measurements of the cavity pattern on the propeller blades are correlated with syncronized measurements of induced pressures on tunnel walls and in the slipstream.

As in the case of uniform flow studies, the facility used for this activity is the Italian Navy cavitation tunnel (CEIMM, see Appendix B), which is characterized by a relatively small test section.

A non-uniform inflow similar to the wake downstream of a single-screw ship hull has been simulated using a wake generator. Two types of wake generators are typically used for similar applications: wire screens and plate arrays. For the present activity, the second option was chosen. In particular, a wake generation device was realized that follows closely the design described by Huse (1996) in the recommendations notes of the International Towing Tank Conference on measurements of hull pressure fluctuations [13].

The set-up realized at the CEIMM cavitation tunnel is sketched in Fig. 7. The wake generator device is composed of five plates spaced 20 mm apart from each other and assembled together to form an array 86 mm thick and 300 mm long. The rack is fixed to the ceiling of the test section, upstream the propeller. A complete description of the wake generator and of the propeller set-up is given in Appendix B.

The inflow to the plate-array can be considered as uniform. The wake generated by the plate-array is measured using a LDV technique (see details in Pereira et al. [15]). In particular, the axial velocity distribution is measured over a transversal plane upstream the propeller at a distance $d = 0.52R_P$ from the propeller disc plane. Two configurations are considered: without propeller (*nominal wake*), and with propeller. In the latter case, the measured velocity field includes both the plate-array wake and the propeller-induced perturbation (*total wake*). No information about the 'effective' wake incoming to the propeller is then available from the present dataset.

All the LDV measurements above are performed at atmospheric pressure, *i.e.,* under cavitation-free conditions.

The two measurements corresponding to upstream velocity $U_\infty = 6.22$ m/s and propeller rotational speed $n = 30.5$ rps are shown in Fig. 8. Measurement points are distributed over a Cartesian grid with some refinement in the region where maximum velocity defect is expected. Due to limitations in the optical access, measurements are not given over a longitudinal stripe on the measurement area. However, such portion is outside the area where the plate-array wake impacts the measurement plane.

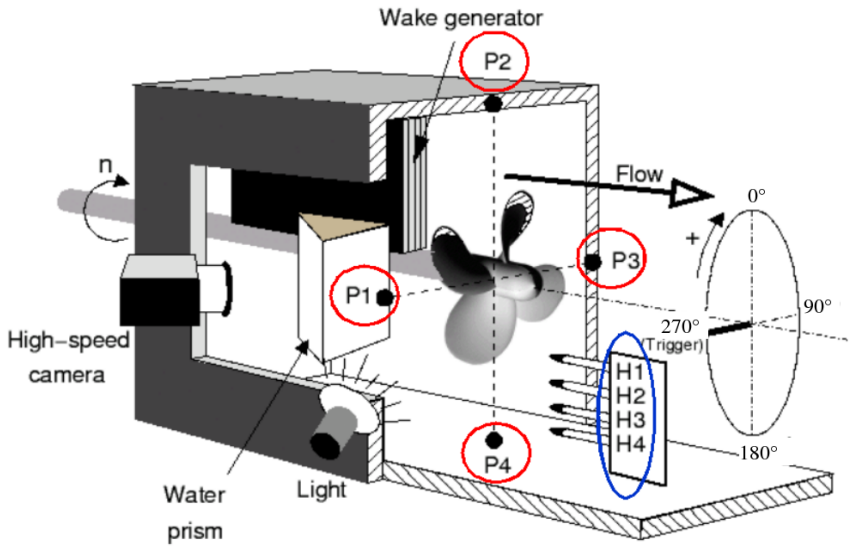

Figure 7: Sketch of the set-up with wake generator, propeller and pressure sensors: pressure transducers (P1, ..P4) and hydrophones (H1, ..H4).

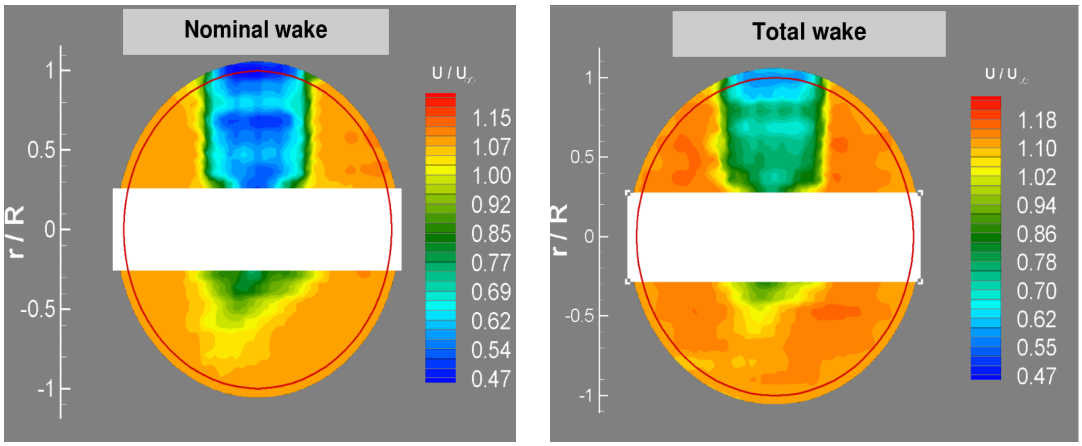

Figure 8: Axial velocity distribution by LDV in the wake generated the plate array. Nominal wake (left) and total wake (right).

Thus, the information given by the LDV analysis is deemed sufficient to adequately characterize the inflow to the propeller.

Figure 8 clearly shows that the plate array generates an intense axial velocity defect that is almost constant within a large portion of the upper half of the propeller disc plane. An approximated averaged value of the velocity defect is $u_x/U_\infty = 0.60$ in the nominal wake, and $u_x/U_\infty = 0.75$ in the total wake, where the propeller suction effect is present. The edges of the wake are very sharp and hence high tangential and radial gradients of the axial velocity are expected.

Testing conditions are adjusted to match thrust identity between propeller in wake field and single propeller in uniform flow as described in Section 3. Specifically, the propeller in wake field is tested at $U_\infty = 6.22$ m/s and $n = 30.5$ rps, which corresponds to $J = 0.897$, and $Re_{0.7R} = 1.40 \times 10^6$ (kinematic viscosity of water $\nu = 1.01 \times 10^{-6}$ m^2/s).

In the above flow conditions at atmospheric tunnel pressure, measured thrust on the propeller gives $K_T = 0.175$, and $K_Q = 0.0334$. From open water curves (towing tank data, see Section 3.1), such loading condition corresponds to a 'thrust-identity' equivalent advance coefficient equal to 0.85, *i.e.*, $J_{O.W.} = 0.85$.

Six different tunnel pressure conditions are considered, corresponding to:

- $\sigma_0 = 2.5, 3.5, 4.5, 5.5, 6.5, 7.5$.

For each flow condition, the following propeller cavitation observations and measurements are documented:

- freestream velocity U_∞ [m/s], propeller rotational speed n [RPS], advance coefficient $J_{O.W.}$, cavitation number σ_n, Reynolds number, $Re_{0.7R}$;
- cavity area A_C for 13 blade angular positions, with angular step of $\Delta\theta = 5^\circ$ (mean value and standard deviation, see Eq. (4));
- high-resolution pictures of blade cavitation;
- pressure signals from 4 pressure transducers flush mounted on tunnel walls and from 4 hydrophones immersed into the propeller slipstream (Fourier harmonics, see Eq. (5)).

Attached cavity area measurements are determined applying the same digital image processing technique used to study the propeller in uniform flow and described by Pereira et al. in [14]. As in the case of the analysis in uniform flow, a reference blade (*key-blade*) is chosen in order to eliminate uncertainty related to different cavity patterns on blades having (small) shape differences. Mean values and standard deviation are calculated over a very large number of samples that are taken when the reference blade is in the same angular position θ.

A total of 13 angular positions is then analysed: $-40^\circ < \theta < 20^\circ$, with $\Delta\theta = 5^\circ$, and $\theta = 0$ corresponding to key blade in the twelve-o'clock position looking from downstream the propeller (see Fig. 7). The angular position of the blade is referred to the blade reference line and is determined through a practical technique in use during model testing that is affected by an uncertainty of $\pm$ 1 degrees.

The distribution of cavity area mean value and standard deviation (see Eq. (4)) as a function of the blade angular position θ and of the cavitation number σ_n is plotted in Fig. 9.

Results in Fig. 9 show that cavity inception and desinence during a revolution occur outside the analysed interval. It may be also noted that even at the highest pressure conditions, $\sigma_0 = 7.5$, a small sheet cavity is present on the blade surface. As a consequence, fully cavitation-free conditions are not documented.

Pressure measurements are performed using both pressure transducers and hydrophones. The set-up is briefly described here, whereas more details are given in [15].

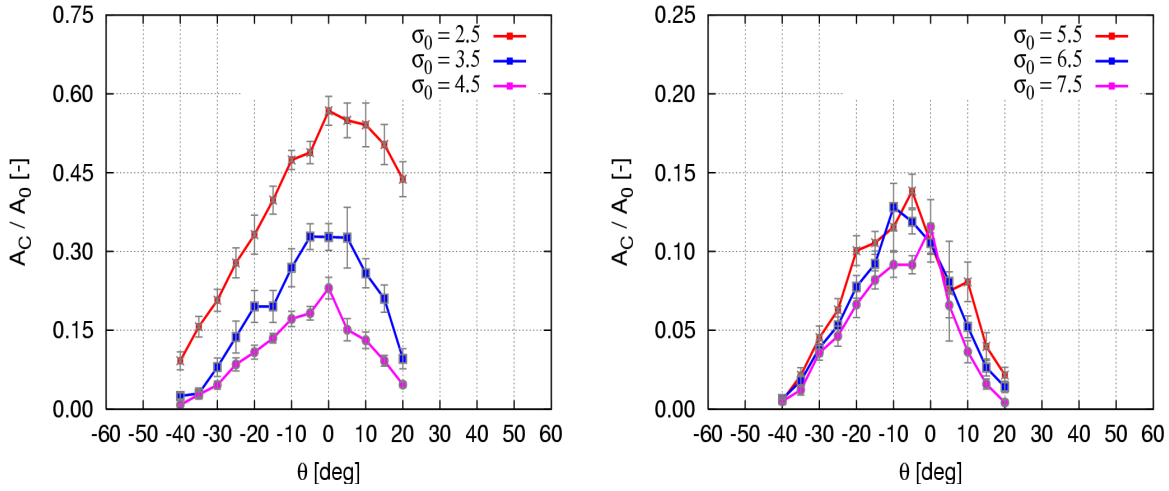

Figure 9: Attached cavity extension (mean value and fluctuations) referred to blade angular position θ: low tunnel pressure conditions (left) and high tunnel pressure conditions (right). Cavity area A_C is presented as a fraction of a blade surface reference area, $A_0 = 0.460 R_P^2$.

Four pressure transducers are flush mounted to the test section walls in correspondence of the propeller disc plane, as indicated in Fig. 7. These pressure transducers are labelled as P1, P2, P3 and P4, and are respectively placed at $\theta = 270°, 0°, 90°, 180°$.

Next, four hydrophones are mounted on a vertical streamlined strut immersed into the propeller slipstream, at distance $x/R_P = 1.0$ from the propeller disc plane (see Fig. 7). The four sensors are labelled as H1, H2, H3, H4, and are located in a radial plane at distance, respectively, $r = 80$ mm, $r = 100$ mm, $r = 120$ mm, and $r = 200$ mm. Sensors H1 and H2 are within the slipstream, H3 is in the propeller tip-vortex region, whereas H4 is in a non-perturbed region and may be used to provide background noise information.

Calibration of both pressure transducers and hydrophones have been performed as described in [15]. Pressure transducers output presents an error between measured and actual pressure levels that is below 0.5% of the full pressure range that can be measured. Hydrophones measurement uncertainty is of ± 1.5 dB re μPa in the range $10 - 80000$ Hz, and a flat frequency response in the range $0.1 - 20000$ Hz with uncertainty of -1.5 to $+1$ dB re μPa.

The pressure and noise signals are sampled at a rate of 100 KHz per channel and recorded for 30 seconds. At a propeller revolution speed of 30 rps, this corresponds to acquisition of one samples from each sensor approximately every $0.11°$ of propeller rotation.

Raw pressure signals are then processed in the frequency domain and Fourier coefficients are determined. By this procedure, high-frequency components related to background noise are filtered.

Denoting by $p(t)$ the time hystory of pressure recorded by any of the 8 sensors, the following equivalent

representations in terms of truncated Fourier series are considered

$$\begin{aligned} \tilde{p}(t) &= \tilde{p}_0(t) + \sum_{k=1}^{N_h} C_k \cos(2\pi k f_{_P} t) + S_k \sin(2\pi k f_{_P} t); \\ \tilde{p}(t) &= \tilde{p}_0(t) + \sum_{k=1}^{N_h} A_k \cos(2\pi k f_{_P} t + \phi_k), \end{aligned} \tag{5}$$

where $f_{_P} = n = 1/T$ denotes the propeller revolution frequency and N_h is the number of harmonics, $\tilde{p}_0(t)$ is the mean pressure averaged through a propeller revolution period, and

$$A_k = \sqrt{C_k^2 + S_k^2}; \qquad \phi_k = -arctan\,(S_k/C_k)\,. \tag{6}$$

The *INSEAN E779A* dataset CD-ROM provides for all the 8 sensors a representation of quantity $\tilde{p}(t) - \tilde{p}_0(t)$ through coefficients C_k, S_k and A_k, ϕ_k (with $k = 1, ...48$, corresponding to $N_h = 48$, in Eqs. (5)).

Using all the 48 coefficients, filtered pressure signals $\tilde{p}(t)$ having a frequency content between about 30 Hz (propeller frequency, $f_{_P}$) and about 1460 Hz are obtained. Different filtering can simply be achieved limiting the number of harmonics that are taken into account in the right-hand side of Eqs. (5).

In view of the large amount of data corresponding to LDV measurements of the propeller wakefield, of cavity pattern and pressure signal measurements, the complete set of data is collected into the *INSEAN E779A* dataset CD-ROM (see Appendix C).

For the sake of completeness, Fourier coefficients of pressure signals from the pressure transducers P1 to P4 are shown in Fig. 10. Specifically, the amplitudes A_k of the first four Propeller Blade Frequency (PBF) harmonics are plotted for six different values of the cavitation number σ_0.

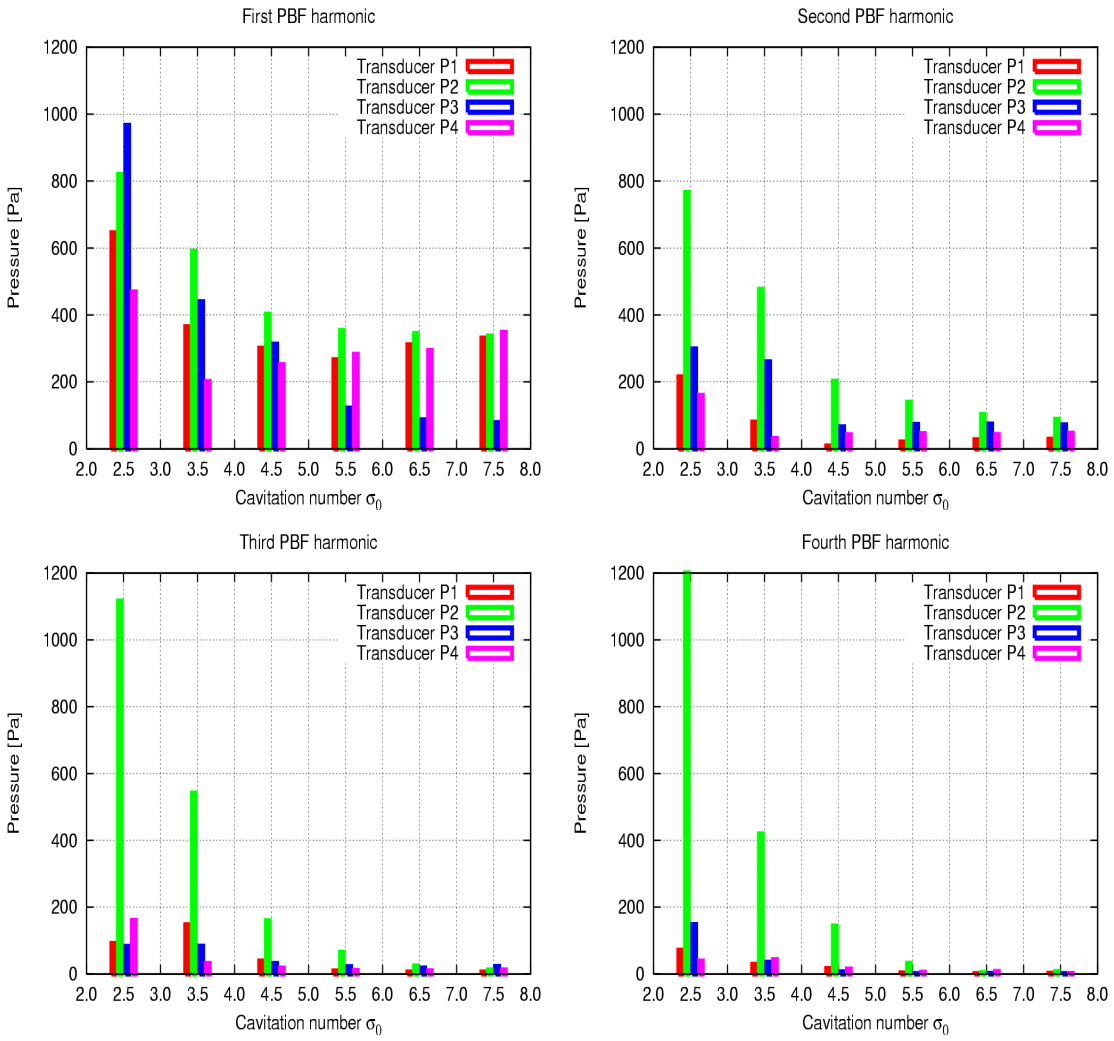

Figure 10: Pressure transducers P1, P2, P3, P4: amplitudes A_k from Eq. 6 for the first four PBF harmonics and $2.5 < \sigma_0 < 7.5$.

References

[1] VIRTUE Project, Work Package 4. 'Review of Existing Datasets for Validation and Selection of Test Cases.' Deliverable D4.1.2, January 2006.

[2] Stella, A., Guj, G., Di Felice, F. (2000). 'Propeller Wake Flowfield Analysis by means of LDV Phase Sampling Techniques. Experiments in Fluids, Vol. 28, pp. 1-10.

[3] Felli M., Tamburini L., Camussi R., Guj G. (2006). 'Analysis of the propeller wake evolution at different blade number by LDV and high speed stereo visualizations. Proceedings of the *12nd Symposium on Flow Visualization,* Goettingen, Germany.

[4] Di Felice F., Romano G.P., Elefante M. (2000). 'Propeller wake analysis by means of PIV.' Proceedings of the *Twenty-third Symposium on Naval Hydrodynamics,* Val de Reuil, France, 2000.

[5] Di Florio, D., Di Felice, F., Romano, G.P, Elefante, M. (2001). "Propeller Wake Structure at Different Advance Coefficients by means of PIV". Proceedings of the *PSFVIP-3,* Maui, Hawaii, U.S.A., March 18-21, 2001.

[6] Di Felice, F., Felli, M., Giordano, G., Soave, M. (2003). "Pressure and Velocity Correlation in the wake of a Propeller". Proceedings of the *Propeller Shafting,* Virginia Beach, Norfolk, September 2003.

[7] Di Felice, F., Di Florio, D., Felli, M., Romano, G.P. (2004). 'Experimental Investigation of the Propeller Wake at Different Loading Conditions by Particle Image Velocimetry.' Journal of Ship Research, Vol. 48, no.2, June 2004, pp. 168-190.

[8] Felli M., Di Felice F., Guj G., Camussi R. (2006). 'Analysis of the Propeller wake evolution by pressure and velocity phase measurements.' Accepted for publication on Experiments in Fluids.

[9] Felli M., Di Florio D., Di Felice F., Calcagno G. (2001). 'Propeller wake visualization by laser anemometry.' Proceedings of the *Sixth Asian Symposium on Visualization,* Pusan, South Korea, 2001

[10] Felli M., Di Florio D., Di Felice F. (2002). 'Comparison between PIV and LDV techniques in the analysis of a propeller wake.' Journal of Visualization, Vol. 5, no.3, 2002.

[11] Glauert, M. A. (1926). 'The Elements of Aerofoil and Airscrew Theory.' Cambridge University Press, London, U.K., 1926.

[12] Report of the Propulsion Committee. Proceedings of the *23rd International Towing tank Conference,* Vol. I. Venice, Italy, September 2002.

[13] Huse, E. (1996). 'Measurements of Hull Pressure Fluctuations.' In: Report of the Specialist Committee on Cavitation. Proceeding of the *21st International Towing Tank Conference,* Vol. I. Trondheim, Norway.

[14] Pereira, F., Salvatore, F., Di Felice, F. (2004). 'Measurement and Modeling of Propeller Cavitation in Uniform Inflow.' Journal of Fluids Engineering, Vol. 126, July 2004, pp. 671-679.

[15] Pereira, F., Salvatore, F., Di Felice, F., Soave, M. (2004). "Experimental Investigation of a Cavitating Propeller in Non-Uniform Inflow". Proceedings of the *25th Symposium On Naval Hydrodynamics,* St. John's, Newfoundland, Canada, August 2004.

A The INSEAN E779A model propeller

The INSEAN E779A is a four-bladed, fixed pitch, right-handed propeller, originally designed in 1959 for a ferry, and never built in full-scale.

Propeller geometrical characteristics are given in Tables 7 to 11.

Propeller diameter	$D_P = 227.27$ mm
Number of blades	$Z = 4$
Pitch ratio (nominal)	$P/D_P = 1.1$
Skew angle at blade tip	$\theta_S^{tip} = 4°48'$ (positive)
Rake (nominal)	$i = 4°35'$ (forward)
Expanded area ratio	$EAR = 0.689$
Hub diameter (at prop. ref. line)	$D_H = 45.53$ mm
Hub length	$L_H = 68.30$ mm

Table 7: Basic geometrical data of the *INSEAN E779A* model propeller.

The model propeller is bronze-made, the hub is tapered and suitable for testing with the propeller driven from upstream. Boss diameter at downstream end is $D_H^{(d)} = 38.3$ mm, at a distance $l_H^{(d)} = 31.9$ mm from the propeller reference line; boss diameter at upstream end is $D_H^{(u)} = 50.9$, at a distance $l_H^{(u)} = 36.4$ mm from the propeller reference line. During model testing with propeller driven from upstream, as in the case of cavitation tunnel tests, a boss cap is mounted downstream the propeller boss. The cap has a parabolic profile, with maximum diameter equal to model propeller boss diameter $D_H^{(d)} = 38.3$ mm, and cap length is equal to 43 mm.

The blade shape is defined through 11 radial sections between $r/R_P = 0.264$ and $r/R_P = 0.9988$.

Blade planform data are given in Table 8, where c is blade chord, x_{LE} and x_{Tmax} denote, respectively, distance of blade leading edge from blade reference line and distance of maximum thickness abscissa from blade reference line; t_{max} is the sectional maximum thickness. The propeller rake is positive if backward (*i.e.*, blade tip away from the ship hull). All quantities in Table 9 are nondimensional.

Blade sectional offsets are given in Tables 9 to 11. Specifically, 28 stations along the chord are considered; chordwise abscissa ξ is defined along the chord, with $\xi = 0$ denoting section leading edge and $\xi = 1$ denoting section trailing edge. Sectional offsets of blade suction side (back) are denoted by y_B, and sectional offsets of blade pressure side (face) are denoted by y_F. Offsets are measured in millimeters and referred to a nominally flat face side: positive as well as negative values of face side offsets and positive values of back side offsets are given.

Propeller blade drawings are given in Fig. 11: expanded outline (left) and developed sectional profiles at correct pitch and rake (right).

Geometrical data described in the present Section have been obtained through a direct measurement of the model propeller using a digital topometry technique. This approach is highly accurate and hence geometrical data reflect the real shape of the propeller model, taking into account both manufacturing and finishing details, as well as shape deviations from original design due to ageing effects.

r/R_P	P/D_P	c/D_P	x_{LE}/D_P	t_{max}/D_P	x_{Tmax}/c	$rake/D_P$
0.2640	1.11179	0.27838	0.16044	0.04033	0.17633	-0.00601
0.3520	1.12039	0.30799	0.17083	0.03124	0.10466	-0.01072
0.4400	1.12021	0.33571	0.18019	0.02565	0.08674	-0.01437
0.5280	1.11671	0.36001	0.18718	0.02119	0.06993	-0.01794
0.6160	1.11467	0.37666	0.18966	0.01672	0.10353	-0.02158
0.7040	1.11728	0.37841	0.18489	0.01293	0.03860	-0.02501
0.7920	1.11738	0.36335	0.16954	0.00967	0.01661	-0.02876
0.8800	1.11024	0.31704	0.13451	0.00626	-0.07573	-0.03267
0.9680	1.11789	0.19174	0.05974	0.00388	-0.18842	-0.03644
0.9900	1.12612	0.11574	0.01621	0.00328	-0.45992	-0.03756
0.9988	1.12612	0.04906	-0.02073	0.00185	-0.97258	-0.03835

Table 8: Blade characteristics of the *INSEAN E779A* model propeller.

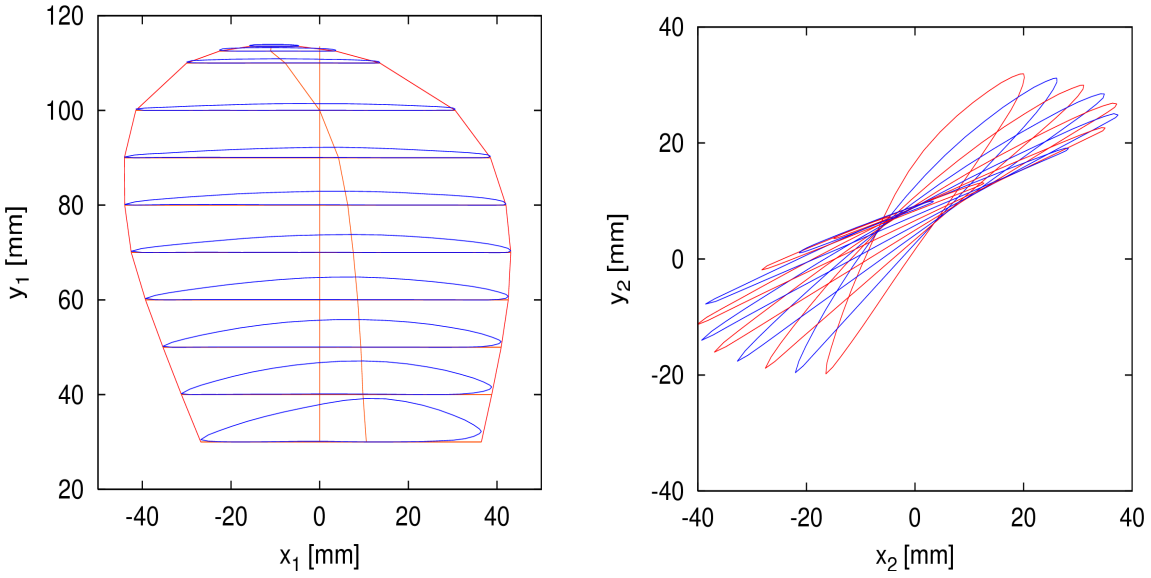

Figure 11: *INSEAN E779A* model propeller drawings. Left: expanded outline; right: developed sectional profiles at correct pitch and rake. Dimensions in millimeters.

r/R_P	ξ	0.00000	0.00625	0.01250	0.02500	0.05000	0.07500	0.10000	0.12500	0.15000	0.20000
0.264	y_B	2.22337	2.74180	3.02267	3.53964	4.38797	5.07529	5.68004	6.23649	6.73942	7.61454
	y_F	2.22337	1.77115	1.55559	1.21831	0.79527	0.53683	0.37259	0.27080	0.20563	0.11372
0.352	y_B	1.60266	1.97140	2.20458	2.61441	3.29985	3.87284	4.35281	4.78321	5.14855	5.79154
	y_F	1.60266	1.13984	0.95193	0.70958	0.40682	0.20746	0.10071	0.02583	0.00590	0.00986
0.440	y_B	1.17964	1.53662	1.73348	2.07872	2.67769	3.17575	3.58729	3.93183	4.23024	4.73823
	y_F	1.17964	0.75759	0.59566	0.38554	0.16147	0.05901	0.01490	0.00535	0.00598	0.00854
0.528	y_B	0.74046	1.15511	1.32917	1.63410	2.13325	2.51687	2.83615	3.10951	3.35455	3.78641
	y_F	0.74046	0.32592	0.22751	0.10423	-0.00519	-0.02163	-0.02012	-0.01568	-0.00630	0.01057
0.616	y_B	0.36094	0.83840	1.00771	1.28202	1.69633	2.02064	2.27855	2.49955	2.70585	3.05037
	y_F	0.36094	0.05945	0.01399	-0.02613	-0.03489	-0.01558	-0.00385	0.00088	0.00456	0.01191
0.704	y_B	0.22176	0.75369	0.90439	1.11976	1.42948	1.65908	1.83894	1.98566	2.11425	2.34379
	y_F	0.22176	0.03216	0.00960	-0.00778	-0.00924	0.00175	0.00762	0.01490	0.02030	0.02094
0.792	y_B	0.30371	0.58787	0.69151	0.84006	1.03059	1.16293	1.26717	1.36635	1.46920	1.67159
	y_F	0.30371	0.04761	0.02878	0.00883	0.00023	0.00094	-0.00183	-0.00356	-0.00385	-0.00281
0.880	y_B	0.27101	0.50153	0.56933	0.64828	0.76362	0.85217	0.93157	1.00550	1.07117	1.18542
	y_F	0.27101	0.06834	0.05186	0.03651	0.02003	0.01349	0.00829	0.00316	0.00175	0.00135
0.968	y_B	0.12791	0.29668	0.35115	0.41291	0.49468	0.55176	0.59980	0.64200	0.67575	0.72629
	y_F	0.12791	0.03156	0.00922	-0.00832	-0.01378	-0.01000	-0.00676	-0.00438	-0.00141	0.00497
0.990	y_B	0.16490	0.26333	0.31066	0.37616	0.45201	0.49898	0.53596	0.56806	0.59201	0.62988
	y_F	0.16490	0.09419	0.07176	0.04605	0.02004	0.00855	0.00283	0.00052	0.00010	0.00310
0.9988	y_B	0.12451	0.16610	0.18382	0.21041	0.24760	0.27478	0.29634	0.31403	0.32922	0.35365
	y_F	0.12451	0.08804	0.07580	0.06024	0.04226	0.03110	0.02339	0.01792	0.01375	0.00834

Table 9: Blade sectional offsets of the *INSEAN E779A* model propeller: Non-dimensional chordwise abscissa ξ, back side offset y_B and face side offset y_F, in millimeters. Chordwise abscissae from $\xi = 0$ to $\xi = 0.2$.

r/R_P	ξ	0.25000	0.30000	0.35000	0.40000	0.45000	0.50000	0.55000	0.60000	0.65000	0.70000
0.264	y_B	8.31395	8.83140	9.13486	9.19303	9.02885	8.69425	8.20057	7.61918	7.01239	6.38812
	y_F	0.05674	0.02063	-0.00195	-0.00384	0.02665	0.08245	0.13659	0.15245	0.13650	0.10218
0.352	y_B	6.29275	6.68757	6.95633	7.09167	7.09881	6.98827	6.77679	6.48293	6.10561	5.63321
	y_F	0.01824	0.05099	0.08217	0.11188	0.13728	0.15484	0.15899	0.14475	0.11934	0.09373
0.440	y_B	5.15209	5.46440	5.68597	5.81210	5.84807	5.80420	5.68020	5.46816	5.16674	4.78305
	y_F	0.01416	0.01864	0.01766	0.02654	0.04616	0.05788	0.06025	0.06130	0.05319	0.04644
0.528	y_B	4.15098	4.44833	4.66341	4.79419	4.84026	4.78735	4.65746	4.45187	4.16175	3.80731
	y_F	0.02148	0.02467	0.02459	0.03270	0.05132	0.05668	0.05480	0.05134	0.04429	0.04167
0.616	y_B	3.32907	3.57356	3.72216	3.79326	3.78665	3.70959	3.60970	3.47437	3.26880	2.98804
	y_F	0.01588	0.00488	0.00647	0.02491	0.04381	0.04933	0.04200	0.02886	0.02517	0.03599
0.704	y_B	2.55960	2.73637	2.86219	2.92950	2.94728	2.90780	2.81541	2.70965	2.57491	2.38786
	y_F	0.01806	0.01966	0.03198	0.05441	0.07558	0.08997	0.09505	0.09033	0.09536	0.10942
0.792	y_B	1.85638	1.99733	2.11360	2.18993	2.20647	2.16724	2.09255	2.00355	1.89094	1.74874
	y_F	0.00376	0.01345	0.03553	0.05762	0.07086	0.07892	0.08293	0.08279	0.08443	0.09183
0.880	y_B	1.28646	1.36007	1.40155	1.41057	1.41510	1.42144	1.40918	1.36459	1.29222	1.19883
	y_F	0.00852	0.01880	0.02645	0.02978	0.03051	0.02900	0.02353	0.01560	0.01153	0.01526
0.968	y_B	0.76908	0.80806	0.84041	0.86351	0.87744	0.88239	0.87965	0.87122	0.85893	0.84098
	y_F	0.01174	0.01874	0.02560	0.03154	0.03585	0.03775	0.03611	0.02951	0.01691	0.00234
0.990	y_B	0.66205	0.68741	0.70524	0.72021	0.73216	0.74091	0.74589	0.74640	0.74171	0.73099
	y_F	0.00844	0.01340	0.01918	0.02355	0.02578	0.02522	0.02210	0.01704	0.01071	0.00454
0.9988	y_B	0.37273	0.38771	0.39943	0.40836	0.41476	0.41871	0.42017	0.41910	0.41531	0.40845
	y_F	0.00497	0.00283	0.00154	0.00081	0.00053	0.00066	0.00116	0.00201	0.00327	0.00517

Table 10: Blade sectional offsets of the *INSEAN E779A* model propeller: Non-dimensional chordwise abscissa ξ, back side offset y_B and face side offset y_F, in millimeters. Chordwise abscissae from $\xi = 0.25$ to $\xi = 0.7$.

r/R_P	ξ	0.75000	0.80000	0.85000	0.90000	0.95000	0.97500	0.98750	1.00000
0.264	y_B	5.70041	4.92748	4.07188	3.12512	2.06086	1.44383	1.08508	0.49052
	y_F	0.04791	0.00216	-0.00585	0.01803	0.09851	0.18119	0.25663	0.49052
0.352	y_B	5.05234	4.35680	3.57424	2.70559	1.70531	1.09951	0.73986	0.20011
	y_F	0.07781	0.06614	0.04648	0.02342	0.00821	0.00648	0.02796	0.20011
0.440	y_B	4.31387	3.74078	3.07590	2.34177	1.49797	0.99030	0.68481	0.18925
	y_F	0.05147	0.05446	0.04465	0.02832	-0.00084	-0.00219	0.01586	0.18925
0.528	y_B	3.40806	2.96379	2.45971	1.92029	1.29937	0.93515	0.72019	0.27661
	y_F	0.04831	0.05980	0.04255	0.00977	0.00567	0.03399	0.07226	0.27661
0.616	y_B	2.66269	2.30714	1.93922	1.53373	1.08749	0.82659	0.66727	0.26882
	y_F	0.04712	0.04823	0.04062	0.01675	0.00971	0.04535	0.08674	0.26882
0.704	y_B	2.14960	1.89141	1.61330	1.31048	0.92514	0.67343	0.52197	0.14577
	y_F	0.11889	0.12798	0.13290	0.10027	0.03785	0.00399	0.00169	0.14577
0.792	y_B	1.58344	1.38967	1.15274	0.94670	0.72847	0.56081	0.45536	0.15625
	y_F	0.10163	0.10750	0.09308	0.06513	0.02408	0.00143	0.00478	0.15625
0.880	y_B	1.08946	0.96977	0.83710	0.69668	0.56462	0.49362	0.43928	0.27412
	y_F	0.01837	0.01430	0.00212	-0.00135	-0.00033	0.00583	0.03239	0.27412
0.968	y_B	0.81306	0.76946	0.71032	0.64157	0.56393	0.50721	0.45011	0.20188
	y_F	-0.00631	-0.00445	-0.00121	0.00259	0.02890	0.05588	0.08439	0.20188
0.990	y_B	0.71366	0.69168	0.66597	0.63197	0.55070	0.47030	0.40585	0.24418
	y_F	0.00153	0.00535	0.01857	0.04247	0.07854	0.10367	0.12973	0.24418
0.9988	y_B	0.39780	0.38258	0.36116	0.33027	0.28230	0.24463	0.21763	0.15818
	y_F	0.00827	0.01331	0.02148	0.03541	0.06136	0.08476	0.10404	0.15818

Table 11: Blade sectional offsets of the *INSEAN E779A* model propeller: Non-dimensional chordwise abscissa ξ, back side offset y_B and face side offset y_F, in millimeters. Chordwise abscissae from $\xi = 0.75$ to $\xi = 1.0$.

B Description of experimental facilities

Two facilities have been used by INSEAN researchers and technicians to perform the experimental analysis collected into the *INSEAN E779A* dataset. Basic characteristics of these facilities are described here below in some detail.

B.1 The towing tank

Open water propeller tests by INSEAN are usually performed in the towing tank No. 2. This is a medium-size longitudial tank, whose characteristics are summarized in Table 12.

length:	220 m.
width:	9.0 m.
depth:	3.5 m., constant
maximum towing carriage speed:	10 m/s

Table 12: Main characteristics of INSEAN Towing Tank No. 2.

The tank is equipped with wave generators for both regular and non-regular wave patterns for seakeeping and ride comfort tests. Main characteristics are: maximum wave length = 10 m, maximum wave height = 0.5 m.

Open water propeller testing is performed mounting the propeller on a streamlined dummy model. The propeller axis depth is 1.5 propeller diameters with respect to calm water free surface level. Propeller rotational speed and towing carriage speed are varied in order to keep the Reynolds number $Re_{0.7R}$ close to 5×10^5, for model propellers of diameter 20-25 cm.

Propeller revolution rate is measured using an optical encoder. Thrust and torque are measured using a REM H29 balance (max. thrust is 392.4 N, max. torque is 147.15 Nm).

B.2 The cavitation tunnel

Most part of the experimental activity documented in the *INSEAN E779A* dataset is carried out at the Italian Navy cavitation facility (CEIMM), located in the area of INSEAN premises.

The tunnel, a Kempf & Remmers closed type circuit, has a $0.6m \times 0.6m \times 2.6m$ square test section, with rounded corners of radius $R_c = 0.10$ m. The resulting nominal cross section area is $A_{tun} = 0.3514$ m^2. Optical access to the test section is possible through large Perspex windows.

Main characteristics are summarized in Table 13.

Propeller testing can be performed using different devices:

- J15 dynamometer: only tests with horizontal propeller shaft are possible
- H40 dynamometer: propeller shaft can be rotated in a vertical plane

test section width and height:	$W_{tun} = H_{tun} = 0.6$ m
geometric test section area	0.3514 m^2 (corner rounding $R_c = 0.10$ m)
test section length:	2.6 m
nozzle contraction ratio:	5.96:1
maximum water speed:	12 m/s
maximum free stream turbulence:	2% (averaged)
	0.6% in the propeller disc area
flow uniformity:	1% (axial vel.); 3% (vertical vel.)
minimum pressure:	0.07 atm
maximum pressure:	1.50 atm

Table 13: Main characteristics of the Italian Navy cavitation tunnel (CEIMM).

In both cases, the propeller is driven upstream. This configuration allows to easily test propeller rudder assemblies.

The inflow to the tunnel test section has been characterized in order to determine the velocity perturbation induced by the wake generated by the balance devices. At standard operating conditions, the turbulence level of the inflow to the test section is between 1.5 and 2.0%. See [2] for details.

B.2.1 Description of wake generator for transient cavitation studies

Non-uniform flow propeller cavitation studies described in Deliverable D4.1.3 have been performed using a wake generator represented by an array of thick plates mounted to the CEIMM tunnel top wall. This kind of set up is described by Huse (1996) in the recommendations notes of the International Towing Tank Conference on measurements of hull pressure fluctuations [13].

The wake generator is depicted in Fig. 12, whereas Figs. 13 provide details of shape and dimensions of the wake generator and of its set-up within the tunnel test section. In bottom Fig. 13, the drawing is qualitative and horizontal and vertical dimensions are not correctly scaled. Only indicated measures are correct.

The tunnel has a test section with square cross section 600 mm wide, whereas the INSEAN E779A model propeller has $D_P = 227.27$ mm. Tunnel corners have rounding radius of 100 mm.

The wake-generator device is composed of five plates spaced 20 mm apart from each other and assembled together to form an array 86 mm thick and 300 mm long. Each plate is 6 mm thick and plate leading and trailing edges are rounded (with 6 mm round-edge diameter). The rack is fixed to the ceiling of the test section, upstream the propeller.

The plates are 232 mm high and are hung to the tunnel ceiling through a a rack. The rack is fixed to the ceiling of the test section, upstream the propeller. The thickness of the rack is 15 mm. Considering that each plate fits into the rack 2 mm deep, the total height of the wake generator including the rack is 245 mm.

There is an extra 30 mm spacer between the wake generator and the ceiling of the test section, which puts the bottom of the wake generator at 275 mm from the top wall. Recalling the tunnel test section is 600 mm high, the propeller/dynamometer shaft axis is 25 mm below the bottom

Figure 12: Tunnel set-up with propeller and wake generator.

of the wake generator. The dynamometer shaft diameter is 45 mm. A fairing ring is fitted on the dynamometer shaft in order to have a smooth transition from shaft diameter to propeller boss diameter. The fairing ring length is 60.0 mm.

The trailing edge of the wake generator plates is located 101 mm upstream the propeller disc plane (corresponding to axial location $x/R_P = -0.89$). The wake generated by the plate array is measured 59 mm upstream the propeller disc plane (corresponding to axial location $x/R_P = -0.52$).

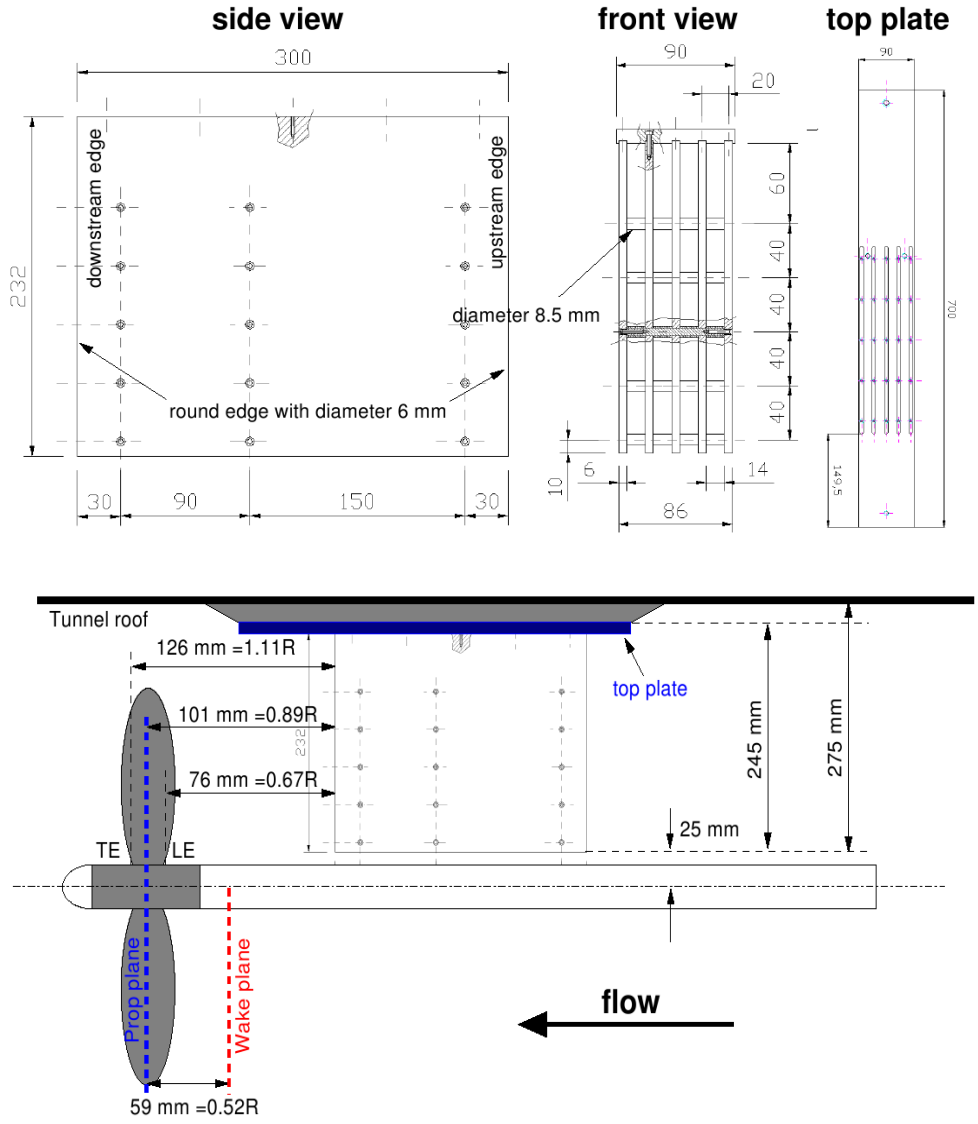

Figure 13: Sketch of wake generator: details of plate rack (top) and set-up with propeller (bottom). The lower drawing is qualitative and horizontal and vertical dimensions are not correctly scaled; only indicated measures are correct.

C The INSEAN E779A Dataset CD-ROM

Part of the data described in the *INSEAN E779A* dataset are provided through a CD-ROM that is given as an annex to the present report.

Reflecting the different flow conditions described in the Report, the CD-ROM content is organized through the following directory tree:

- E779A Geometry
  - Standard tables and IGES file
- E779A Uniform Flow
  - Open Water
  - Slipstream Flow by LDV
  - Slipstream Flow by PIV
  - E779A Steady Cavitation
    - Pattern Photo at J=0.71
    - Pattern Photo at J=0.77
    - Pattern Photo at J=0.83
- E779A Non Uniform Flow
  - Inflow by LDV
  - Unsteady Cavitation (J=0.90)
    - Pattern Photo at Sigma=2.50
    - Pattern Photo at Sigma=3.50
    - Pattern Photo at Sigma=4.50
    - Pattern Photo at Sigma=5.50
    - Pattern Photo at Sigma=6.50
    - Pattern Photo at Sigma=7.50
  - E779A Pressure Fluctuations
    - Fourier Coefficients
- E779A Reports

All data are stored in files of different format:

- Text files (extensions 'TXT' and 'COF')
- MS-Office Excel spreadsheet (extension 'XLS')
- Photoghaphs (extensions 'TIF' and 'JPG')
- Velocimetry raw data, formatted files (extensions 'DAT')

- Velocimetry contour plot files for TECPLOT© (extensions 'LAY' and 'PLT')

Reference should be made to the present Report to have a complete explaination of the meaning of physical quantities provided, of conventions used etc.